Magnetic Resonance Imaging 58 (2019) 32–37

Contents lists available at ScienceDirect

Magnetic Resonance Imaging

journal homepage: www.elsevier.com/locate/mri

Original contribution

Susceptibility weighted MRI after uterine artery embolization for leiomyoma

Yasuyuki Yamahana[a,*], Tetsuya Katsumori[b], Hiroshi Miura[a], Shunsuke Asai[a], Sachimi Yamada[a], Akiko Takahata[a], Kei Yamada[a]

[a] Department of Radiology, Kyoto Prefectural University of Medicine, 465 Kajii-cho, Kamigyo-ku, Kyoto 602-8566, Japan
[b] Department of Radiology, Saiseikai Shiga Hospital, Ohashi 2-4-1, Ritto, Shiga 520-3046, Japan

ARTICLE INFO

Keywords:
Magnetic resonance imaging
Uterine artery embolization
Leiomyoma
Fibroid
Uterus
Suceptibility weighted imaging

ABSTRACT

Purpose: To evaluate whether susceptibility-weighted MR imaging (SWI) findings are associated with tumor infarction on contrast-enhanced MRI (CE-MRI) after uterine artery embolization (UAE) for leiomyoma.

Methods: This was a single institution, retrospective study. Between February 2016 and April 2017, 27 consecutive patients underwent UAE and completed SWI and CE-MRI before and 1 week after UAE. Two blinded readers independently reviewed the MRI of 261 tumors ≥1 cm in all patients. We evaluated the relationship between the hypointense peripheral rim observed on the tumor surface on post-procedural SWI and the infarction rates (≥90%, < 90%) of each tumor based on post-procedural CE-MRI. Inter-reader correlation coefficients (ICC) and the sensitivity and specificity of the rim were measured.

Results: Substantial inter-reader agreement was noted in post-procedural SWI interpretations (ICC = 0.681, 95% CI; 0.547, 0.771). The rim was observed in 66.7% (174/261) of tumors by reader 1 and 55.9% (146/261) of tumors by reader 2 on post-procedural SWI. Correlations were observed between the rim and ≥90% tumor infarction by readers 1 and 2 (Spearman's coefficient = 0.474 and 0.438, $p < 0.001$ and $p < 0.001$, respectively). The sensitivity and specificity of the rim to tumor infarction were 77.2 and 82.6% (reader 1), and 65.8 and 100% (reader 2), respectively.

Conclusions: The present study demonstrated that the hypointense peripheral rim was observed on some leiomyomas on SWI immediately after UAE. The rim correlated with tumor infarction on post-procedural CE-MRI. This SWI finding was helpful for evaluating embolic effects on leiomyomas in the acute phase after UAE.

1. Introduction

Uterine artery embolization (UAE) is regarded as a safe and effective therapy for symptomatic uterine leiomyoma. This minimally invasive procedure induces tumor infarction, leading to tumor reductions and the amelioration of symptoms in most patients [1,2]. Tumor infarction after UAE is considered to be an important predictor affecting the duration of symptom control in the long term [3–5].

MRI is an established imaging modality for the evaluation of uterine leiomyoma [3–12]. Previous MRI studies revealed that tumor infarction after UAE observed on MRI corresponded to hemorrhagic infarction (i.e., red degeneration) [6–9]. The MRI features of leiomyoma treated by UAE were reported to have the appearance of a "bag of blood-products", namely, a high signal intensity on T1-weighted images (T1WI) and homogeneous low signal intensity on T2-weighted images (T2WI) [6–9].

Contrast-enhanced MRI (CE-MRI) is the gold standard imaging tool for evaluating tumor infarction after UAE [3–7,13,14]. However, CE-MRI is not indicated for some patients who are contraindicated to use contrast material. Additionally, contrast material has been associated with the potential deposition of gadolinium in the brain [15]. Therefore, a new imaging tool that requires no contrast material and provides useful information on tumor infarction is desired.

With the rapid development of MRI technology, susceptibility-weighted imaging (SWI) has been attracting attention for cerebral diseases [16], but is poorly documented in gynecological disorders [17,18]. SWI findings of leiomyoma after UAE have yet to be reported. Since SWI is a useful imaging modality for detecting blood products, showing as signal voids [17,18], we hypothesized that SWI may be applicable to the evaluation of leiomyoma after UAE. In our preliminary review of SWI, we found a specific finding, a hypointense peripheral rim, on the surface of some leiomyomas with hemorrhagic

* Corresponding author.
E-mail address: yamahana@koto.kpu-m.ac.jp (Y. Yamahana).

https://doi.org/10.1016/j.mri.2019.01.013
Received 21 September 2018; Received in revised form 13 January 2019; Accepted 14 January 2019

infarction immediately after UAE. Therefore, we speculated that this SWI finding may correlate with embolic effects on tumors after UAE.

The primary aim of the present study was to investigate whether SWI findings on uterine leiomyoma immediately after UAE are associated with tumor infarction on post-procedural CE-MRI.

2. Material and methods

This was a single institution, retrospective study approved by the Institutional Review Board. Written informed consent for the procedure and subsequent follow-up and opt-out consent for the retrospective use of data were obtained from all patients. No funding for the present study was received from any companies or organizations.

All data used for the present study were obtained from electronic medical records, a database on UAE for leiomyoma in the institution, or a retrospective interpretation of MRI.

2.1. Study population

Between February 2016 and April 2017, 43 consecutive patients were referred to the Department of Radiology in the institution to undergo UAE for symptomatic uterine leiomyomas. Inclusion criteria for the procedure included premenopausal women aged 20 years or older with uterine leiomyomas causing symptoms including menorrhagia, pain, or bulk-related symptoms. We did not place any upper limit on the volume of uterine leiomyomas or the uterus. Pedunculated subserosal leiomyomas or co-existing adenomyosis unlikely to be related to symptoms were included. Exclusion criteria for the procedure included the presence of a gynecological malignancy in the examination before UAE, an undiagnosed pelvic mass, acute pelvic infection, coagulopathy, pregnancy, menopause, contraindications to MRI, an allergy to iodinated contrast medium or gadolinium, dominant adenomyosis mainly causing symptoms, and dominant infarcted leiomyoma.

Twelve out of the 43 patients referred were excluded from UAE: six had better treatment options than UAE, four declined UAE after counselling, one had breast cancer, which was noted after counselling, and one had a desire to treat infertility by UAE. Therefore, 31 patients underwent UAE as the primary treatment in the institution. Additionally, 4 out of the 31 patients were excluded from the present study: two did not undergo SWI because they had baseline MRI before the present study, one had a history of UAE, which potentially affects tumor infarction, and one did not undergo CE-MRI 1 week after UAE due to an allergy to gadolinium, which was caused by the administration of gadolinium for CE-MRI before UAE. As a result, 27 out of the 31 patients were included in the present study.

Baseline characteristics were as follows. Mean age was 43.8 ± 4.4 years (standard deviation, SD) (range, 34–51 years), mean body weight was 58.0 ± 14.4 kg (SD) (range, 43–105 kg), and the mean body mass index was 22.9 ± 5.2 (SD) (range, 18.5–39.3). Eighteen women were nulliparous. The mean number of tumors that were 1 cm or larger per patient was 9.7 ± 8.9 (SD) (range, 1–31). The mean volume of the dominant tumor was 429 ± 290 ml (SD) (range, 38–1317 ml), while the mean volume of the uterus was 1064 ± 504 ml (SD) (range, 202–2792 ml).

2.2. UAE technique

Ten out of the 27 procedures were performed by an experienced interventional radiologist and the remaining 17 procedures with the same method by two qualified interventional radiologists under the supervision of the unique operator. A microcatheter was coaxially advanced through a 5 Fr catheter into the horizontal portion of the uterine artery. Thereafter, 500–900 μm tris-acryl gelatin microspheres (Embosphere, Nippon Kayaku, Tokyo, Japan) were infused under fluoroscopic guidance. No other embolic agents (e.g., gelatin sponge particles) were used in any patient. The angiographic endpoint was defined as the complete obstruction of the peri-fibroid plexus and sluggish flow in the ascending portion of the uterine arteries.

2.3. MRI

All patients underwent MRI with a 1.5 T unit (SIGNA Explorer, GE Healthcare, Connecticut, US) at baseline and 1 week after UAE. Axial T1WI, axial and sagittal T2WI, axial diffusion-weighted imaging (DWI), axial SWI, and axial and sagittal contrast-enhanced T1WI (i.e., CE-MRI) were performed.

Axial SWI was acquired with the 3D SWAN, T2*-weighted 3D-gradient echo pulse sequence, consisting of magnitude and phase images. The parameters used were as follows: TR/TE, 62.4/50.0 ms; slice thickness, 6 mm; intersection gap, 0 mm; flip angle, 15 degrees; matrix, 352 × 224; field of view, 25 cm; total imaging time, 113 s. Axial CE-MRI was obtained with fast spin echo (TR/TE, 440/14.4 ms; slice thickness, 6 mm; intersection gap, 1 mm; flip angle, 160 degrees; matrix, 320 × 192; field of view, 25 cm; total imaging time, 113 s) after the intravenous administration of 0.1 mol/kg of gadobutrol (Gadovist, Bayer, Berlin, Germany).

2.4. Image analysis

One reader with > 10 years' experience of pelvic MRI reviewed the baseline T2WI of 27 patients, selected 261 tumors that were 1 cm or larger, and then numbered each tumor. Thereafter, two blinded readers with > 10 years' experience of pelvic MRI independently reviewed axial CE-MRI before and 1 week after UAE, referring to baseline T2WI. Tumor infarction was defined as the absence of enhancement on CE-MRI. The two readers individually evaluated the rate of the infarction volume to the total tumor volume of each tumor with CE-MRI 1 week after UAE followed by CE-MRI at baseline. They then categorized these rates into two grades: complete to nearly complete tumor infarction (≥ 90%) and partial to no tumor infarction (< 90%) [5].

After an 8-week interval following the interpretation of CE-MRI, in order to reduce a recall bias, the same two readers individually reviewed axial SWI obtained 1 week after UAE followed by axial SWI at baseline, referring to baseline T2WI, under the blinding of CE-MRI results. Before the interpretation, they discussed the definition of the hypointense peripheral rim with a review of several SWI obtained after May 2017 with the same protocol in our hospital (apart from the subjects of the present study), and reached a consensus on the definition of the rim as follows: (1) the proportion of the surface area of the hypointense peripheral rim to the total surface area of each leiomyoma was subjectively divided into three grades with all slices of axial SWI: complete (100–70%), partial (69–30%), and no rim (29–0%); (2) the degree of the thickness of the rim was not considered to be a criterion for judgements on the presence or absence of the rim; (3) the hypointense peripheral rim was defined when it was possible to distinguish it from intra-tumor characteristics, even those for hypointense tumors; and (4) if the hypointense area was inside the surface, it was not considered to be a hypointense peripheral rim. The two readers then investigated the hypointense peripheral rim on the surface of the tumor (Figs. 1 and 2) and categorized it into the three grades.

2.5. Study aim

The primary endpoint was the correlation between the hypointense peripheral rim on SWI 1 week after UAE and tumor infarction on CE-MRI 1 week after UAE. The secondary endpoints were the sensitivity, specificity, and accuracy of the rim to ≥ 90% tumor infarction as well as the optimal cut-off threshold of the rim for the prediction of ≥ 90% tumor infarction.

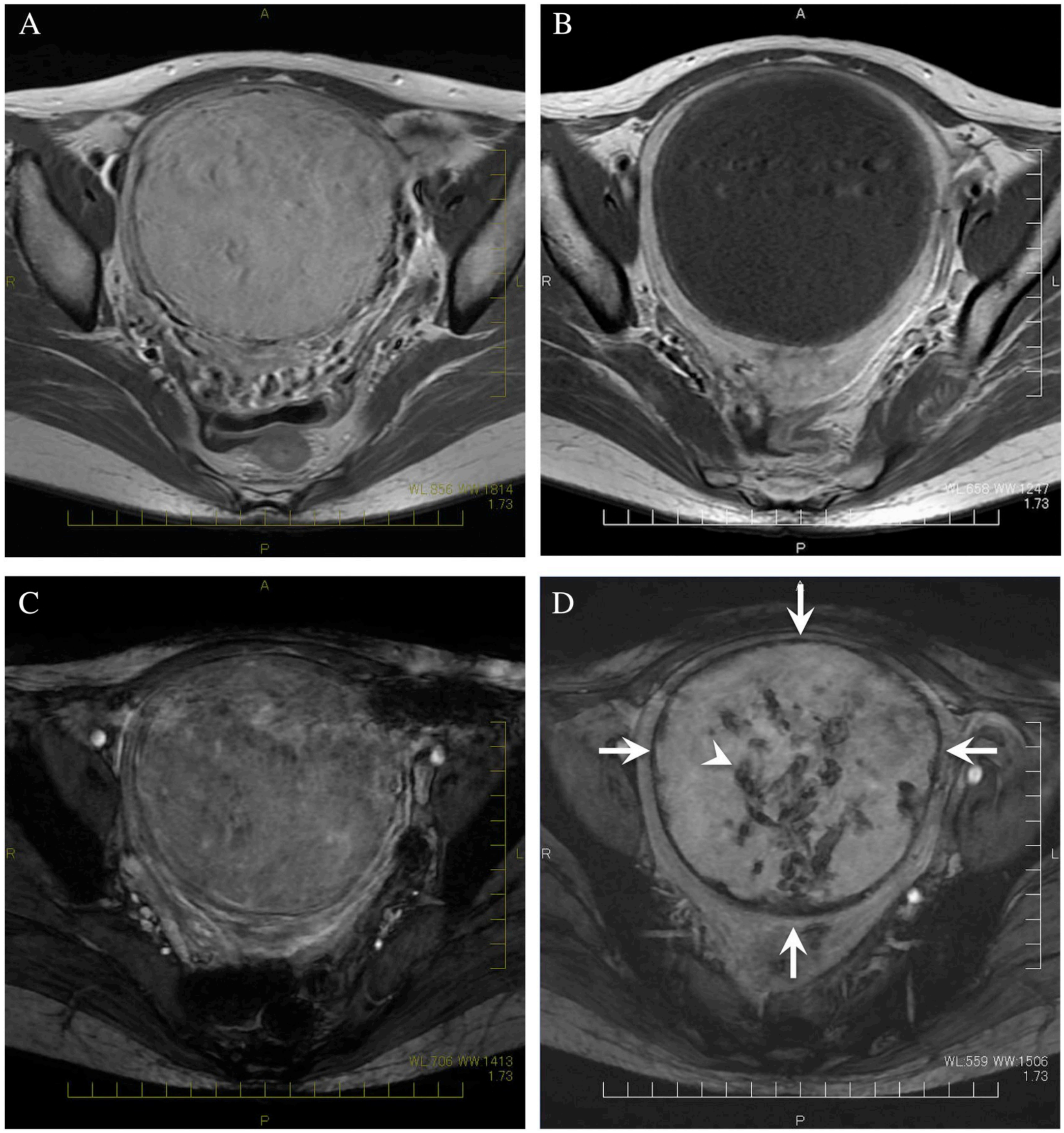

Fig. 1. A 49-year-old woman with uterine leiomyoma.
A. Contrast-enhanced T1-weighted image obtained before UAE showing a well-enhanced tumor.
B. Contrast-enhanced T1-weighted image obtained 1 week after UAE showing that the tumor was not enhanced.
C. Susceptibility-weighted image obtained before UAE showing no hypointense peripheral rim on the tumor surface.
D. Susceptibility-weighted image obtained 1 week after UAE showing a complete peripheral hypointense rim (arrows) and punctate signal void (arrow head) in embolized leiomyoma.

2.6. Statistical analysis

Inter-reader correlation coefficients (ICC) regarding tumor infarction (≥90% or < 90%) on CE-MRI 1 week after UAE and the frequencies of ≥90% tumor infarction were measured. ICC regarding the hypointense peripheral rim in the interpretations of post-procedural SWI were calculated. The frequencies of the hypointense peripheral rim on SWI before and after UAE were measured and compared with Wilcoxon's test. An ICC value of < 0 was considered to indicate a poor agreement; 0–0.20, a slight agreement; 0.21–0.40, a fair agreement; 0.41–0.60, a moderate agreement; 0.61–0.80, a substantial agreement; 0.81–1, an almost perfect agreement [19].

The relationship between the hypointense peripheral rim on post-procedural SWI and ≥90% tumor infarction on CE-MRI after UAE was assessed with Spearman's rank correlation. Spearman's coefficient value of 0 was considered to indicate no correlation; 0.2, a weakly positive correlation; 0.5, a moderately positive correlation; 0.8, a strongly positive correlation; 1.0, a perfectly positive correlation [20].

The sensitivity, specificity, and accuracy of the hypointense peripheral rim on post-procedural SWI to ≥90% tumor infarction on CE-MRI after UAE were calculated at each cut-off threshold of the rim, and the optimal cut-off threshold of the rim for the prediction of ≥90% tumor infarction was then assessed. Statistical analyses were performed with SPSS software (version 25; IBM, Armonk, NY). P-values of < 0.05 were considered to be significant.

3. Results

All patients successfully underwent UAE. The mean follow-up period after UAE was 8.5 ± 3.3 months (SD) (range 3–15 months). No patients underwent additional surgery after UAE during the period of the present study. All patients underwent planned MRI including SWI and CE-MRI at baseline and 1 week after UAE.

ICC for tumor infarction on CE-MRI 1 week after UAE corresponded

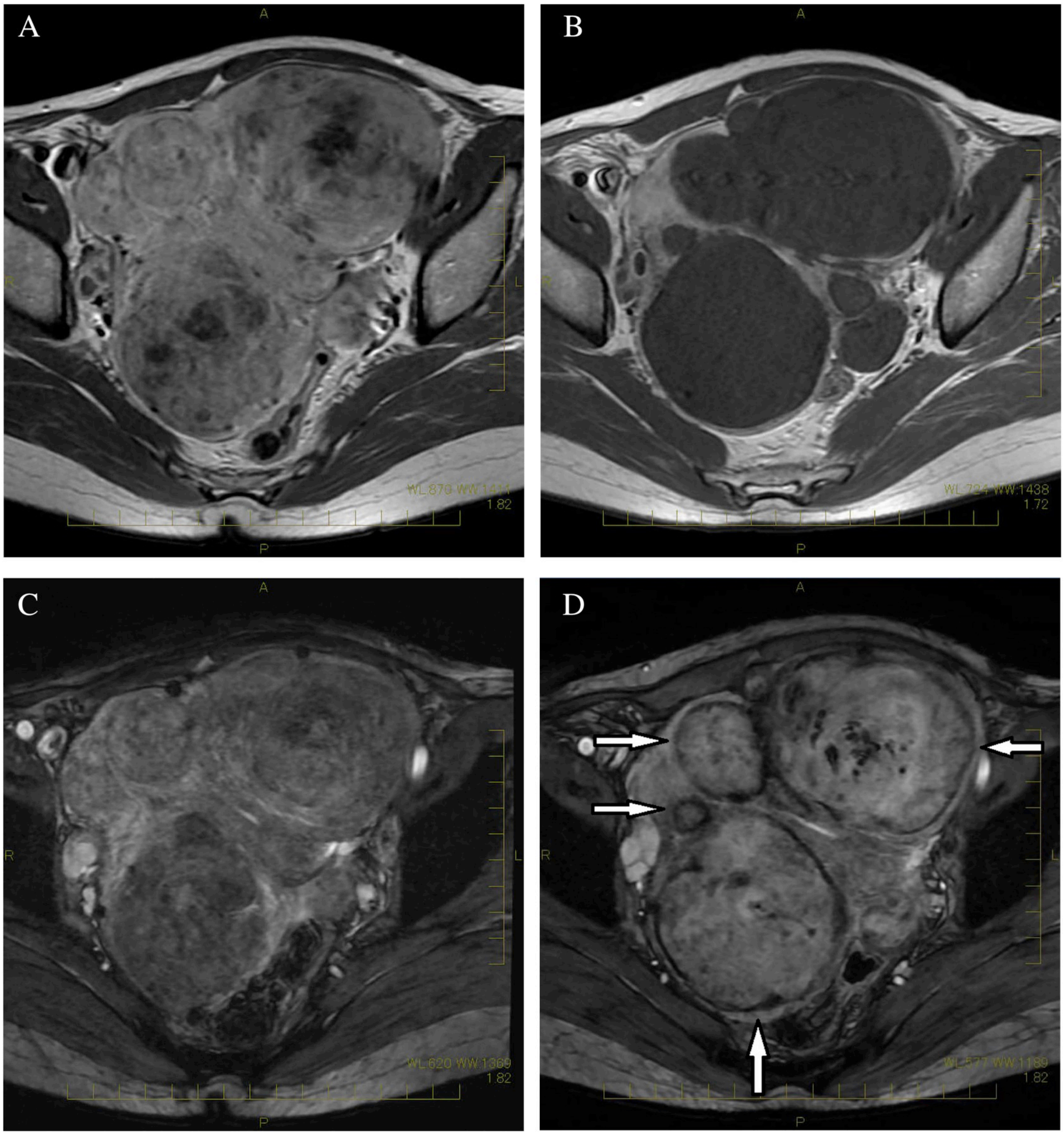

Fig. 2. A 45-year-old woman with multiple uterine leiomyomas.
A. Contrast-enhanced T1-weighted image obtained before UAE showing multiple well-enhanced leiomyomas.
B. Contrast-enhanced T1-weighted image obtained 1 week after UAE showing that tumors (arrows) were not enhanced, corresponding to complete infarction.
C. Susceptibility-weighted image obtained before UAE showing no peripheral hypointense rim on the surface of each tumor.
D. Susceptibility-weighted image obtained 1 week after UAE showing that tumors with complete infarction had a complete peripheral hypointense rim (arrows).

to a substantial agreement (0.622, 95% CI; 0.542, 0.691). Ninety percent or higher tumor infarction was observed in 82.4% (215/261) of tumors by reader 1 and 85.1% (222/261) of tumors by reader 2 (Table 1). ICC regarding the hypointense peripheral rim on SWI 1 week after UAE corresponded to a substantial agreement (0.681, 95% CI; 0.547, 0.771).

A complete or partial hypointense peripheral rim on SWI at baseline was observed in 3.8% (10/261, 7 complete rims and 3 partial rims) of tumors by reader 1 and 3.1% (8/261, 3 complete rims and 5 partial rims) of tumors by reader 2; whereas a complete or partial rim on SWI immediately after UAE was noted in 66.7% (174/261, 142 complete rims and 32 partial rims) of tumors by reader 1 and 55.9% (146/261, 96 complete rims and 50 partial rims) of tumors by reader 2 (Tables 1 and 2). The frequencies of the complete or partial hypointense peripheral rim were significantly higher than those at baseline ($p < 0.001$; reader 1, $p < 0.001$; reader 2, Table 2).

The correlation between the hypointense peripheral rim and tumor infarction on CE-MRI after UAE was significant by readers 1 and 2 (Spearman's coefficient = 0.474 and 0.438, $p < 0.001$ and $p < 0.001$, respectively, Table 3, Fig. 2).

When the cut-off threshold of the hypointense peripheral rim was defined between a partial rim and no rim, the sensitivity, specificity, and accuracy of the hypointense peripheral rim to ≥90% tumor infarction on CE-MRI after UAE were 77.2, 82.6, and 78.2% by reader 1 and 65.8, 100, and 70.9% by reader 2, respectively (Tables 1 and 4). When the cut-off threshold of the hypointense peripheral rim was defined between a complete rim and partial rim, the sensitivity, specificity, and accuracy of the rim to ≥90% tumor infarction on CE-MRI after UAE were 64.7, 91.3, and 69.3% by reader 1 and 43.2, 100, and 51.7% by reader 2, respectively. These results suggested that the optimal cut-off threshold of the hypointense peripheral rim was between a partial rim and no rim for the prediction of ≥90% tumor infarction.

4. Discussion

To the best of our knowledge, the present study is the first to report

Table 1
Relationship between a hypointense peripheral rim on SWI 1 week after UAE and tumor infarction on CE-MRI 1 week after UAE.

Reader 1

		SWI			
		Hypointense peripheral rim			
		Complete	Partial	No	Total
CE-MRI	≥90% tumor infarction	138	28	49	215
	< 90% tumor infarction	4	4	38	46
	Total	142	32	87	261

Reader 2

		SWI			
		Hypointense peripheral rim			
		Complete	Partial	No	Total
CE-MRI	≥90% tumor infarction	95	51	76	222
	< 90% tumor infarction	0	0	39	39
	Total	95	51	115	261

SWI = susceptibility-weighted MR imaging.
UAE = uterine artery embolization.
CE-MRI = contrast-enhanced MRI.

Table 2
Frequency of a hypointense peripheral rim on SWI.

	SWI at baseline	SWI 1 week after UAE	p-Value[a]
Reader 1	3.8% (10/261)	66.7% (174/261)	< 0.001
Reader 2	3.1% (8/261)	55.9% (146/261)	< 0.001

The hypointense peripheral rim corresponded to a complete or partial rim.
SWI = susceptibility-weighted MR imaging.
UAE = uterine artery embolization.
[a] Wilcoxon's test.

Table 3
Spearman's rank correlation between a hypointense peripheral rim on SWI 1 week after UAE and ≥90% tumor infarction on CE-MRI 1 week after UAE.

	Coefficient	p-Value
Reader 1	0.474	< 0.001
Reader 2	0.438	< 0.001

SWI = susceptibility-weighted MR imaging.
UAE = uterine artery embolization.
CE-MRI = contrast-enhanced MR.

Table 4
Sensitivity and specificity of a hypointense peripheral rim on SWI 1 week after UAE to ≥90% tumor infarction on CE-MRI 1 week after UAE.

	Reader 1	Reader 2
Sensitivity (%)	77.2	65.8
Specificity (%)	82.6	100
Accuracy (%)	78.2	70.9
Positive predictive value (%)	95.4	100
Negative predictive value (%)	43.7	33.9
Positive likelihood ratio	4.43	NA
Negative likelihood ratio	0.28	0.34

The hypointense peripheral rim corresponded to a complete or partial rim.
SWI = susceptibility-weighted MR imaging.
UAE = uterine artery embolization.
CE-MRI = contrast-enhanced MRI NA = not available.

SWI findings after UAE for leiomyoma. This study revealed a major result. SWI immediately after UAE provided a specific finding, namely, a hypointense peripheral rim, which was poorly observed before UAE. Most importantly, the hypointense peripheral rim was associated with tumor infarction on CE-MRI after UAE. The SWI findings may be helpful for evaluating imaging outcomes, i.e., tumor infarction, and contribute to clinical practice, including counselling and follow-up after UAE. The sensitivity and specificity of the hypointense peripheral rim to tumor infarction were acceptable because these values were similar to those reported previously, in which MRI findings (tumor intensity on baseline T1WI, T2WI, or DWI) were associated with MRI imaging outcomes (tumor reductions) after UAE [21–24].

There are several MR sequences currently used for evaluating leiomyoma infarction after UAE. T1WI and T2WI after UAE provide some findings of blood products in embolized tumors; however, evaluating the degree of tumor infarction after UAE is challenging [6–9]. DWI is also a useful sequence for evaluating tumor infarction 6 months after UAE, as previously reported, but not for assessing tumor infarction in the acute phase after UAE [14]. CE-MRI is regarded as the gold standard imaging tool for evaluating tumor infarction after UAE [3–7,13,14]. This sequence is useful in the acute phase (the next day to 1 week) and chronic phase (after several months) following UAE [3–7,13,14,25]. However, if contrast media is not used, the evaluation of leiomyoma infarction with CE-MRI is challenging. In comparison with these conventional MRI, as shown in the present study, SWI allows evaluation of tumor infarction in the acute phase without the use of contrast media, especially for patients in whom contrast media are contraindicated. SWI is also superior to CE-MRI in that the potential deposition of gadolinium in the brain is avoided [15]. However, it remains unclear which one of SWI or CE-MRI is more appropriate for evaluating tumor infarction in the acute phase after UAE. Therefore, we consider that further investigation is required to address this question, particularly if SWI is routinely used instead of CE-MRI in all patients.

We investigated MRI (including SWI and CE-MRI) obtained 1 week after UAE in the present study. Previous studies performed CE-MRI in the acute phase, i.e., the next day to 1 week after UAE, in order to evaluate tumor infarction, blood flow in the myometrium, and ischemia of the uterus [4,5,14,25]. Furthermore, they reported that tumor infarction on CE-MRI in the acute phase after UAE was associated with subsequent imaging and clinical outcomes [4,5,14,25]. Therefore, we considered MRI obtained 1 week after UAE to be a justified method for evaluating embolic effects on leiomyomas after UAE.

MRI several months after UAE may be desirable in clinical practice [3,6,7,14,21–24]. However, in our preliminary review with SWI obtained 4 months after UAE, we were unable to identify any specific findings associated with tumor infarction. Thus, we did not focus on SWI several months after UAE in the present study. If SWI in the chronic phase after UAE needs to be evaluated, another study may be warranted.

The hypointense peripheral rim is an issue that needs to be addressed. Several MRI studies revealed that leiomyoma infarction induced by UAE suggested hemorrhagic infarction [6–9]. MRI characteristics have been reported to have the appearance of blood products, i.e., a high signal intensity on T1WI and homogeneous low signal intensity on T2WI [6–9]. Since SWI is a useful sequence to demonstrate acute hemorrhage, intravascular clots, and previous microbleeds [17,18], we hypothesize that the hypointense peripheral rim on SWI may correspond to acute thrombosis (hemosiderin or deoxyhemoglobin deposition) in embolized vessels on the surface of a tumor, based on previous findings [17,26]. However, previous pathological studies showed that leiomyoma after UAE was diagnosed as coagulative or hyaline necrosis [27–29]. It currently remains unclear whether hemosiderin or deoxyhemoglobin deposition occurs pathologically on the surface of leiomyoma after UAE [27–29]. Accordingly, further studies to investigate histopathological and radiological correlations may be required. Since all patients in the present study successfully underwent UAE, no pathological investigation after additional surgery following UAE was performed.

There were some limitations in the present study. This was a retrospective study with a limited number of cases. Furthermore, the hypointense peripheral rim on SWI only provided information on the tumor surface, and did not always represent the whole tumor. However, the present study demonstrated a correlation between the rim on SWI and tumor infarction on CE-MRI. Additionally, the rim and tumor infarction were evaluated with a subjective method for each reader. This may have induced a potential bias. Another limitation was that ICC regarding the interpretation of CE-MRI and SWI corresponded to a substantial agreement. This was a potential bias for the present results. Markedly higher values may be optimal for excellent reproducibility.

5. Conclusions

The present study demonstrated that a hypointense peripheral rim on the tumor surface was present on some uterine leiomyomas on SWI immediately after UAE. The rim correlated with tumor infarction on post-procedural CE-MRI. This SWI finding was helpful for evaluating embolic effects on leiomyomas in the acute phase after UAE.

Declaration of interest statement

Tetsuya Katsumori has received honoraria for lectures and writing a manuscript in a journal from Nippon Kayaku, Tokyo, Japan. And Kei Yamada has received honorarium for lectures from Bayer, Osaka, Japan. The payments are not related to the present manuscript. The other authors declare that they have no conflict of interest.

References

[1] van Overhagen H, Reekers JA. Uterine artery embolization for symptomatic leiomyomata. Cardiovasc Intervent Radiol 2015;38:536–42.
[2] Dariushnia SR, Nikolic B, Stokes LS, et al. Society of Interventional Radiology Standards of Practice Committee. Quality improvement guidelines for uterine artery embolization for symptomatic leiomyomata. J Vasc Interv Radiol 2014;25:1737–47.
[3] Pelage JP, Guaou NG, Jha RC, Ascher SM, Spies JB. Uterine fibroid tumors: long-term MR imaging outcome after embolization. Radiology 2004;230:803–9.
[4] Katsumori T, Kasahara T, Kin Y, Nozaki T. Infarction of uterine fibroids after embolization: relationship between postprocedural enhanced MRI findings and long-term clinical outcomes. Cardiovasc Intervent Radiol 2008;31:66–72.
[5] Kroencke TJ, Scheurig C, Poellinger A, Gronewold M, Hamm B. Uterine artery embolization for leiomyomas: percentage of infarction predicts clinical outcome. Radiology 2010;255:834–41.
[6] Burn PR, McCall JM, Chinn RJ, Vashisht A, Smith JR, Healy JC. Uterine fibroleiomyoma: MR imaging appearances before and after embolization of uterine arteries. Radiology 2000;214:729–34.
[7] Jha RC, Ascher SM, Imaoka I, Spies JB. Symptomatic fibroleiomyomata: MR imaging of the uterus before and after uterine arterial embolization. Radiology 2000;217:228–35.
[8] Verma SK, Gonsalves CF, Baltarowich OH, Mitchell DG, Lev-Toaff AS, Bergin D. Spectrum of imaging findings on MRI and CT after uterine artery embolization. Abdom Imaging 2010;35:118–28.
[9] Deshmukh SP, Gonsalves CF, Guglielmo FF, Mitchell DG. Role of MR imaging of uterine leiomyomas before and after embolization. Radiographics 2012;32:251–81.
[10] Kawakami S, Togashi K, Konishi I, et al. Red degeneration of uterine leiomyoma: MR appearance. J Comput Assist Tomogr 1994;18:925–8.
[11] Ueda H, Togashi K, Konishi I, et al. Unusual appearances of uterine leiomyomas: MR imaging findings and their histopathologic backgrounds. Radiographics 1999;19:131–45.
[12] Nakai G, Yamada T, Hamada T, et al. Pathological findings of uterine tumors preoperatively diagnosed as red degeneration of leiomyoma by MRI. Abdom Radiol 2017;42:1825–31.
[13] Katsumori T, Nakajima K, Tokuhiro M. Gadolinium-enhanced MR imaging in the evaluation of uterine fibroids treated with uterine artery embolization. AJR Am J Roentgenol 2001;177:303–7.
[14] Sutter O, Soyer P, Shotar E, et al. Diffusion-weighted MR imaging of uterine leiomyomas following uterine artery embolization. Eur Radiol 2016;26:3558–70.
[15] McDonald RJ, McDonald JS, Kallmes DF, et al. Gadolinium deposition in human brain tissues after contrast-enhanced MR imaging in adult patients without intracranial abnormalities. Radiology 2017;285:546–54.
[16] Zivadinov R, Ramasamy DP, Benedict RR, et al. Cerebral microbleeds in multiple sclerosis evaluated on susceptibility-weighted images and quantitative susceptibility maps: a case-control study. Radiology 2016;281:884–95.
[17] Takeuchi M, Matsuzaki K, Nishitani H. Susceptibility-weighted MRI of endometrioma: preliminary results. AJR Am J Roentgenol 2008;191:1366–70.
[18] Takeuchi M, Matsuzaki K. Adenomyosis: usual and unusual imaging manifestations, pitfalls, and problem-solving MR imaging techniques. Radiographics 2011;31:99–115.
[19] Landis JR, Koch GG. The measurement of observer agreement for categorical data. Biometrics 1977;33:159–74.
[20] Kundel HL, Polansky M. Measurement of observer agreement. Radiology 2003;228:303–8.
[21] Duvnjak S, Ravn P, Green A, Andersen PE. Magnetic resonance signal intensity ratio measurement before uterine artery embolization: ability to predict fibroid size reduction. Cardiovasc Intervent Radiol 2017;40:1839–44.
[22] Kang SH, Lee SJ, Jeon GS, Yoon SW. Scaled signal intensity of uterine fibroids on T2-weighted MR imaging as a predictor of the potential response to uterine fibroid embolization. J Vasc Interv Radiol 2017;28:844–9.
[23] Hecht EM, Do RK, Kang SK, Bennett GL, Babb JS, Clark TW. Diffusion-weighted imaging for prediction of volumetric response of leiomyomas following uterine artery embolization: a preliminary study. J Magn Reson Imaging 2011;33:641–6.
[24] Noda Y, Kanematsu M, Goshima S, et al. Prediction of early response to uterine artery embolization in fibroids: value of MR signal intensity ratio. Magn Reson Imaging 2015;33:51–5.
[25] Ruuskanen A, Sipola P, Hippeläinen M, Wüstefeld M, Manninen H. Pain after uterine fibroid embolization is associated with the severity of myometrial ischaemia on magnetic resonance imaging. Eur Radiol 2009;19:2977–85.
[26] Pelage JP, Le Dref O, Beregi JP, et al. Limited uterine artery embolization with tris-acryl gelatin microspheres for uterine fibroids. J Vasc Interv Radiol 2003;14:15–20.
[27] Colgan TJ, Pron G, Mocarski EJ, Bennett JD, Asch MR, Common A. Pathologic features of uteri and leiomyomas following uterine artery embolization for leiomyomas. Am J Surg Pathol 2003;27:167–77.
[28] Dundr P, Mára M, Masková J, Fucíková Z, Povỳsil C, Tvrdík D. Pathological findings of uterine leiomyomas and adenomyosis following uterine artery embolization. Pathol Res Pract 2006;202:721–9.
[29] Weichert W, Denkert C, Gauruder-Burmester A, et al. Uterine arterial embolization with tris-acryl gelatin microspheres: a histopathologic evaluation. Am J Surg Pathol 2005;29:955–6.